Available online at www.sciencedirect.com
SCIENCE DIRECT®
ELSEVIER
Thin-Walled Structures 41 (2003) 973–986
THIN-WALLED STRUCTURES
www.elsevier.com/locate/tws

Robust control of a vibrating plate using μ-synthesis approach

P. Li [a,b], L. Cheng [a,*], Y.Y. Li [a], N. Chen [b]

[a] *Department of Mechanical Engineering, The Hong Kong Polytechnic University, Hung Hom, Kowloon, Hong Kong SAR, People's Republic of China*
[b] *Department of Mechanical Engineering, Southeast University, Nan Jing 210096, People's Republic of China*

Received 26 September 2002; received in revised form 28 January 2003; accepted 18 March 2003

Abstract

In this paper, the use of μ-synthesis technique for the vibration control of plate-like structures is investigated. First, a robust μ-controller is synthesized and the selection of weightings is discussed. Different from the conventional studies, the mathematical model between the disturbance force and the structure is not required during the controller design. A MIMO control system is built using dSPACE DS1103 platform. Then, MIMO experimental tests are performed. A H_∞ controller with same weightings is also designed and implemented for comparison purpose. Small masses are added to the structure to simulate parameter variations for the robustness investigation. Experimental results show that μ-controller can provide good disturbance rejection in the analyzed bandwidth and is more robust to parameter variations than H_∞ controller. The experimental findings of the present study using a MIMO μ-synthesis scheme are believed to be useful for the vibration control of more general thin-walled structures.

Keywords: Robust control; Plate vibration; μ-Synthesis; H_∞ control; Parameter variation; Weighting function

* Corresponding author. Tel.: +852-2766-6769; fax: +852-2365-4703.
E-mail address: mmlcheng@polyu.edu.hk (L. Cheng).

0263-8231/$ - see front matter © 2003 Elsevier Ltd. All rights reserved.
doi:10.1016/S0263-8231(03)00049-1

1. Introduction

Robust vibration control of plate-like structures has received much attention due to their wide applications, and led to a rapid development of various control strategies such as the LQG control and the fuzzy control, etc. [1–3]. In recent years, a great deal of attention has been paid to the H_∞ control because it not only provides a unified and general control framework for all control structures, but also yields a controller with guaranteed margins [4,5]. However, H_∞ control models all uncertainties as a single complex full block, which results in a rather conservative design [6]. Under such circumstances, the μ-synthesis technique, which involves the use of H_∞ optimization for synthesis and structured singular value (μ) for analysis, has been developed [7–9]. Literature survey shows that most results related to μ-synthesis are simulations or SISO experimental tests. For MIMO cases, only a few results have been reported, e.g. the results of Balas and Doyle [10,11]. Due to the coupling between different sensors and actuators, the design of MIMO controllers is significantly more complex and demanding than the SISO case in terms of control performance, stability and robustness. Up to this point, there is no sufficient experimental evidence using MIMO scheme for vibration suppression using μ-synthesis.

Prior to the MIMO control implementation, the synthesis of a μ-controller is needed. During the controller design, an issue to be considered is the process of the mathematical model between the disturbance force and the structure, which is always assumed to be known [7–9,12]. In engineering practice, however, it is difficult to obtain this model even through system identification or theoretical approach. Hence, how to design a μ-controller without requiring a mathematical model between the disturbance force and the structure is of great interest in the application of μ-synthesis technique.

The aim of this paper is to design such a μ-controller and to verify its robustness by performing MIMO experiments. These investigations would hopefully provide additional experimental evidence to the existing literature for a better assessment of the μ-synthesis control. The outline of this paper is as follows. Section 2 presents the design of a robust μ-controller and the selection of performance and uncertainty weighting functions. In Section 3, the MIMO experimental tests are carried out based on the dSPACE DS1103 PPC digital system, and some additive masses added to the plate to simulate parameter variation for the robustness investigation. For comparison purposes, a H_∞ controller with same weightings is also implemented and compared to the μ-synthesis control. Finally, some conclusions are drawn.

2. Robust μ-control design

In general, the design of a μ-control system includes the synthesis of the controller and the selection of weighting functions. The consideration of the physical system is crucial. The so-called physical system includes both the system to be controlled and the actuator/sensor configuration. Different selections of actuator/sensor locations lead to very different sensor/actuator transfer functions and accordingly

affect the design of μ-controllers. As is known, the actuator/sensor configuration determines the controllability and observability of the system, which has direct impact on the modes to be controlled and the control energy required [13,14]. When piezoelectric actuators are used, they should be usually located at regions where the strain deformations of the most dominant modes are large enough. Ideally, sensors should be collocated (or at least very close to the actuators) to ensure the plant model described by the transfer function as a minimum phase system in the controlled frequency band. The number of sensors and actuators to be used depends on the number of modes to be controlled.

2.1. Synthesis of the μ-controller

A block diagram of a μ-control system design is shown in Fig. 1. $C(s)$ is the plant model described by the transfer function matrix between the control force $u(t)$ and the sensor. $\Delta C(s)$ is the plant uncertainty module including the unmodeled dynamics, parameter variations and the error of system identification, and is described as the multiplicative uncertainty in the frequency region. $K(s)$ is the controller. $P(s)$ is the transfer function matrix between the disturbance force $F(t)$ and the sensor, which is difficult to be determined in practice. Using modal analysis, the mathematical model of the structure is expressed as

$$\begin{cases} \ddot{q}_i + 2\omega_i\zeta_i\dot{q}_i + \omega_i^2 q_i = \sum_{k=1}^{M} u_{ik}(t)\phi_i(x_k^u, y_k^u, z_k^u), \quad i = 1,...,n \\ y_l = \sum_{i=1}^{n} \phi_i(x_l^a, y_l^a, z_l^a)\ddot{q}_i + e_{1,l}, \quad l = 1,...,N \end{cases}, \tag{1}$$

where q_i, $\phi_i(x,y,z)$, ω_i and ζ_i are the modal coordinate, shape function, natural fre-

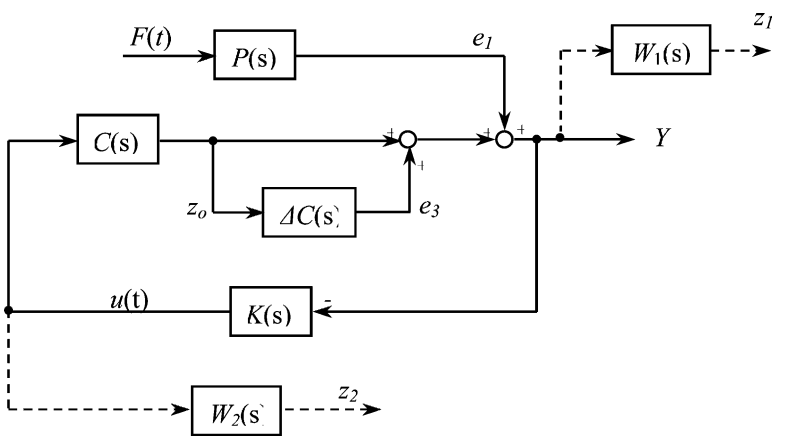

Fig. 1. Block diagram of a robust μ-control system.

quency and damping ratio of mode i, respectively. (x_k^u,y_k^u,z_k^u) and (x_l^a,y_l^a,z_l^a) are locations of the kth actuator and the lth sensor, respectively. $u_{ik}(t)$ is the kth control force acting on the ith mode, and $e_{1,l}$ is the response of the lth sensor to the disturbance. Transforming Eq. (1) into the state-space form by introducing state vectors $X_c = [\{q\}^T\{\dot{q}\}^T]^T$ and $e_1 = \{e_{1,1},...,e_{1,N}\}^T$ yields

$$\begin{cases} \dot{X}_c = \mathbf{A}_c X_c + \mathbf{B}_c u(t) \\ Y = \mathbf{C}_c \dot{X}_c + e_1 = \mathbf{C}_c \mathbf{A}_c X_c + \mathbf{C}_c \mathbf{B}_c u(t) + e_1 \end{cases}, \tag{2}$$

where

$$\mathbf{A}_c = \begin{bmatrix} \mathbf{0}_{n\times n} & \mathbf{I}_{n\times n} \\ -\mathbf{K}_A & -\mathbf{C}_A \end{bmatrix},\ \mathbf{B}_c = \begin{bmatrix} \mathbf{0}_{n\times M} \\ \mathbf{B}_{n\times M} \end{bmatrix},\ \mathbf{C}_c = [\mathbf{0}_{N\times n}\ \ \mathbf{C}_{N\times n}],\ \mathbf{K}_A = \begin{bmatrix} \omega_1^2 & & \\ & \ddots & \\ & & \omega_n^2 \end{bmatrix}_{n\times n},$$

$$\mathbf{C}_A = \begin{bmatrix} 2\zeta_1\omega_1 & & \\ & \ddots & \\ & & 2\zeta_n\omega_n \end{bmatrix}_{n\times n},\ \mathbf{B} = \begin{bmatrix} \phi_1(x_1^u,y_1^u,z_1^u) & \dots & \phi_1(x_M^u,y_M^u,z_M^u) \\ \dots & \dots & \dots \\ \phi_n(x_1^u,y_1^u,z_1^u) & \dots & \phi_n(x_M^u,y_M^u,z_M^u) \end{bmatrix}_{n\times M},$$

$$\mathbf{C} = \begin{bmatrix} \phi_1(x_1^a,y_1^a,z_1^a) & \dots & \phi_n(x_1^a,y_1^a,z_1^a) \\ \dots & \dots & \dots \\ \phi_1(x_N^a,y_N^a,z_N^a) & \dots & \phi_n(x_N^a,y_N^a,z_N^a) \end{bmatrix}.$$

For the μ-synthesis control, the objective is to design a controller $K(s)$ satisfying the following constraint with the presence of plant uncertainty $\Delta C(s)$

$$\|T_{Ye_1}(s)\|_\infty = \|[1 + (1 + \Delta C(s))C(s)K(s)]^{-1}\|_\infty < 1, \tag{3}$$

where $Y_{e_1}(s)$ is the transfer function matrix between e_1 and Y. In general, in order to find a controller to suppress e_1 in desired frequency bandwidth, Y should be weighted by a performance weighting function matrix $W_1(s)$. In addition, the control force $u(t)$ should be weighted by the uncertainty weighting function matrix $W_2(s)$ so as to prevent the saturation of controller output. Thus, the control objective, i.e. Eq. (3), should be rewritten as

$$\left\| \begin{matrix} T_{z_1e_1}(s) \\ T_{z_2e_1}(s) \end{matrix} \right\|_\infty = \left\| \begin{matrix} W_1(s)[1 + (1 + \Delta C(s))C(s)K(s)]^{-1} \\ W_2(s)K(s)[1 + (1 + \Delta C(s))C(s)K(s)]^{-1} \end{matrix} \right\|_\infty < 1, \tag{4}$$

where $z_1 = W_1(s)Y$, $z_2 = W_2(s)u(t) = W_2(s)K(s)Y$.

In order to apply the general μ-framework [15] to the AVC design, the plant uncertainty $\Delta C(s)$ is represented by $\Delta C(s) = \Delta_3(s)W_3(s)$, with $\|\Delta_3(s)\|_\infty \leq 1$. $W_3(s)$ is the robust weighting function. By introducing a fictitious uncertainty block $\Delta_F = [\Delta_{F1}\Delta_{F2}](\|\Delta F\|_\infty \leq 1)$ between the disturbance e_1 and control objects $[z_1\ z_2]^T$, i.e. $e_1 = \Delta_F[z_1\ z_2]^T$, an augmented AVC system in the general μ-framework is given (see Fig. 2) as

$$\begin{bmatrix} z_1 \\ z_2 \\ z_3 \\ Y \end{bmatrix} = \begin{bmatrix} W_1(s) & W_1(s) & W_1(s)C(s) \\ 0 & 0 & W_2(s) \\ 0 & 0 & W_3(s)C(s) \\ 1 & 1 & C(s) \end{bmatrix} \begin{bmatrix} e_1 \\ e_3 \\ u \end{bmatrix} = \hat{G}_P(s) \begin{bmatrix} e_1 \\ e_3 \\ u \end{bmatrix}. \tag{5}$$

In the general μ-framework, the control problem (Eq. (4)) is to find a stable $K(s)$ so that the closed-loop system is stable for all model uncertainty $\Delta_3(s)$ and its infinity-norm is less than 1, i.e.

$$\left\| \begin{matrix} T_{z_1e_1}(s) \\ T_{z_2e_1}(s) \end{matrix} \right\|_\infty = \left\| \begin{matrix} W_1(s)[1 + (1 + \Delta C(s))C(s)K(s)]^{-1} \\ W_2(s)K(s)[1 + (1 + \Delta C(s))C(s)K(s)]^{-1} \end{matrix} \right\|_\infty \tag{6}$$

$$= \|F_U(F_L(\hat{G}_P(s),K(s)),\Delta_3)\|_\infty \leq 1,$$

where F_L and F_U are the lower and upper linear fractional transformation, respectively [15]. Thus, the problem is equivalent to find a $K(s)$ which the inequality

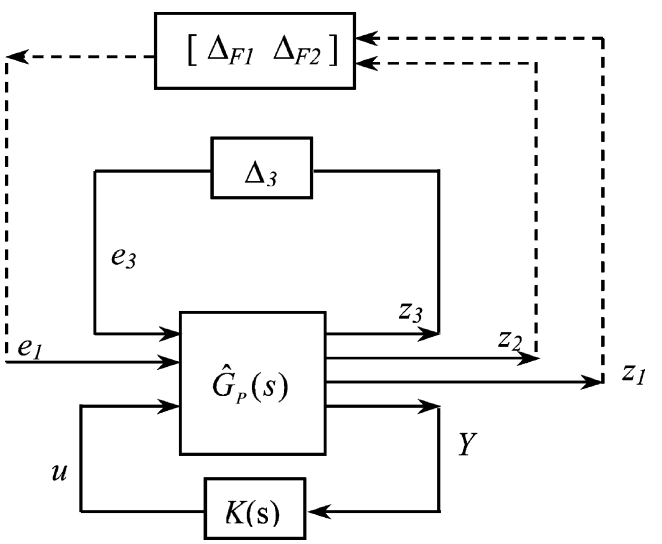

Fig. 2. An augmented AVC system.

$$\sup_{\omega\in R}\mu(\hat{G}(j\omega)) = \sup_{\omega\in R}\mu(F_{\mathrm{L}}(\hat{G}_P(j\omega),K(j\omega))) < 1 \tag{7}$$

holds under the constrain

$$\left\| \begin{matrix} T_{z_1e_1}(s) \\ T_{z_2e_1}(s) \end{matrix} \right\|_\infty = \|F_{\mathrm{U}}(F_{\mathrm{L}}(\hat{G}_P,K),\Delta_3)\|_\infty \leq 1.$$

Obviously, this is the *standard μ-control problem*, and the design can be based on the MATLAB μ-toolbox, in which the *D-K* iteration is adopted to perform the synthesis procedure. D-K iteration is a two-step minimization process: the first step is a minimization of the H_∞ norm over all stabilizing controllers K while the scaling matrix D is held fixed, and the second step is a minimization over a set of scaling D while the controller K is held fixed [16,17].

2.2. Selection of weighting functions

As is known, the weightings are included in controller synthesis instead of in control system implementation to yield robust performance and stability. In general, in order to find a controller, they should be properly selected in advance.

As shown in Fig. 1, with open loop, i.e. $K(s) = 0$, the transfer function matrix $T_{YF}(s) = [1 + (1 + \Delta C(s))C(s)K(s)]^{-1}P(s)$ is simply $P(s)$. Hence, the reduction of the principal gains of $T_{YF}(s)$ using feedback control can result in the disturbance rejection. It is clear that when the disturbance force $F(t)$ is an impulse, $P(s)$ and $T_{YF}(s)$ will be the open- and closed-loop frequency response matrices at outputs Y, respectively. Since the resonance peaks in the frequency response matrix are a measure of damping for each mode, the constraint of $|T_{YF}(s)|_\infty < 1$ can be regarded as a closed-loop damping constraint on the structure modes. Although $P(s)$ is not always available in engineering practice, it shows the essence of the control mechanism. Based on this fact, the control objective, i.e. $\|T_{Ye_1}(s)\|_\infty < 1$ in Eq. (3), is also interpreted as a closed-loop damping constraint on the structure modes. Thus, the selected $W_1(s)$ should be intended to penalize the resonant peaks only, in which those modes that make dominant effects in structural vibration should be weighted maximally.

3. Experimental analyses

3.1. Experimental setup

The structure used for vibration control is an aluminum plate with dimensions of $380 \times 300 \times 3$ mm^3. The plate is clamped on the left side and fixed by two screws on the right side on the workbench (see Fig. 3). Three pairs of PZT patches with dimensions of $50 \times 50 \times 0.5$ mm^3 (Sensortec BM500) are bonded on the two opposite sides of the plate using the adhesive (Loctite 495). PZT-3 is used to generate disturb-

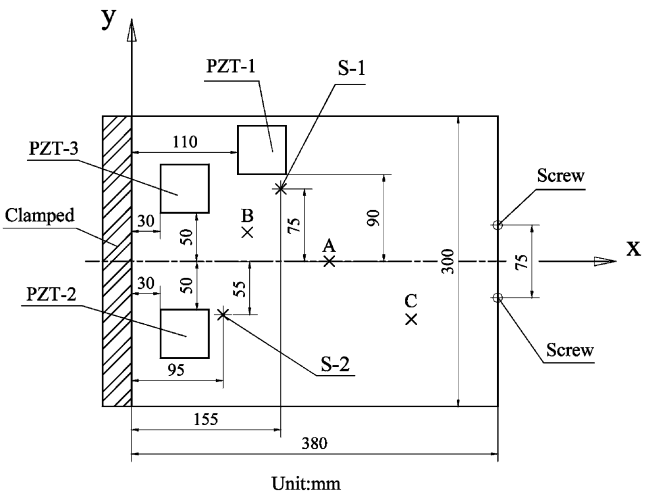

Fig. 3. The tested plate.

ance while PZT-1 and PZT-2 are used as actuators to provide control actions. The experimental setup is shown schematically in Fig. 4. The responses of the plate are monitored by two accelerometers (B&K 4369) at locations S-1 and S-2. Signals are then amplified (using B&K 2635), filtered (using band-pass filter, YE-3790), and fed to a digital control system. The 2×2 control algorithms are implemented using dSPACE DS1103 system with necessary Matlab/Simulink software installed in a PC. A dual-channel power amplifier (Trek Model 700) is used to amplify the control signals. Disturbance is created using white noise generated from the DS1103. Low-pass filters are used to prevent exciting the structure beyond the control bandwidth and to smooth the control signal. Band-pass filters are used to suppress the effect of unmodeled dynamics on the controller design and prevent aliasing. Since the frequency band to be controlled is between 0 and 200 Hz including the first five

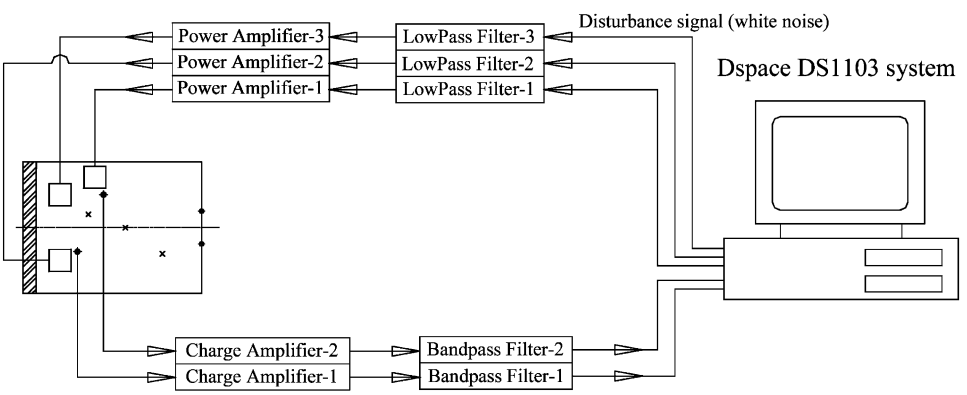

Fig. 4. Schematic diagram of experimental setup.

modes of the plate, the cut-off frequency of low-pass filter is set to 200 Hz, and the frequency range of band-pass filter is from 5 to 200 Hz to exclude the instability caused by the accelerometer in low-frequency (<5 Hz). The sampling rate of DS1103 is selected to be 500 Hz. The control objective is to minimize the power spectrum density of two sensor outputs within the control bandwidth under the excitation of the disturbance force.

The plate described above is just one of the many other possible configurations. The implementation of sensors and actuators is based on the general principle given in Section 2. The selected PZT/accelerometer locations can properly cover the first five modes, while ensuring a minimum phase system $C(s)$ in the controlled frequency band by keeping accelerometers close to the PZT actuators.

3.2. System identification of the plant model C(s)

The synthesis of the μ-controller is based on a nominal model $C(s)$ constructed by low-frequency modes. Thus, the identification of $C(s)$ is the first step of the design. In the present case, a *five-mode multivariable model* of plate structure is used. During the system identification, a sample rate of 500 Hz is adopted for data acquisition. *Hanning window* and *ensemble average* are utilized to enhance the quality of data. In addition, the Chebyshev polynomial is employed to fit the transfer function. The *first five* nature frequencies and the corresponding damping ratios are identified and tabulated in Table 1.

3.3. Selection of weighting function matrices

The determination of weighting function matrices $W_1(s)$, $W_2(s)$ and $W_3(s)$ is a crucial step in the controller design. As mentioned in Section 2.2, the introduction of $W_1(s)$ is to reduce the influence of disturbance on sensor outputs. In general, it is chosen with large amplitude so as to suppress the low-frequency vibration. In this paper, $W_1(s)$ is chosen as a two-order diagonal matrix, and each diagonal element is given by

$$w_1(s) = As^2 \prod_{i=1}^{5} \frac{1}{(s^2 + 2\sigma_i\omega_i s + \omega_i^2)}, \tag{8}$$

Table 1
The first five natural frequencies and damping ratios

Mode	Natural frequency (Hz)	Damping ratio (%)
1	56.6	0.28
2	68.8	0.38
3	121.1	0.10
4	146.5	0.17
5	180.2	0.67

where $A = 5\times10^{21}$, $\sigma_1 = 0.03$, $\sigma_2 = 0.04$, $\sigma_3 = 0.02$, $\sigma_4 = 0.01$ and $\sigma_5 = 0.0015$. Fig. 5 shows the amplitude-frequency response of $w_1(s)$. The above selection of $W_1(s)$ for each accelerometer channel penalizes all the first five lower frequency modes which are in the control bandwidth 0–200 Hz.

The weighting function matrix $W_2(s)$ is selected as

$$W_2(s) = \begin{bmatrix} 0.1 & 0 \\ 0 & 0.1 \end{bmatrix}$$

to prevent the saturation of controller output due to the ±10 V limits of DS1103 D/A converter output.

The robust weighting function matrix $W_3(s)$ is selected to be

$$W_3(s) = \frac{2s + 400}{3s + 2000}\begin{bmatrix} 1 & 0 \\ 0 & 1 \end{bmatrix}. \tag{9}$$

It is clear that the four elements of the transfer function matrix $C(s)$ have the same weight. This weight implies that the model error is approximately 20% at lower frequency that rises to approximately 60% at high frequency (200 Hz). Fig. 5 shows the amplitude-frequency response of $W_1(s)$ and $W_3(s)$. Since $W_2(s)$ has a constant magnitude of 0.1, it is not shown in the figure. It should be emphasized that this uncertainty weight is only the predicted uncertainty values rather than the true uncertainty values which are obviously unknown. As in the case of this weight, the closed-loop system will be robust to 20% error at low-frequency rising to 60% at high frequency.

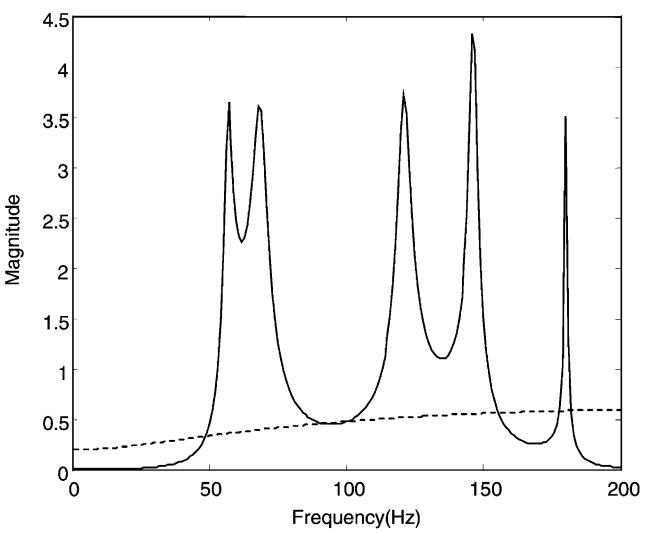

Fig. 5. Frequency response of weightings: $W_1(s)$, ————; $W_3(s)$, -----.

3.4. Experimental results

Using these weighting function matrices, *five D-K* iterations are performed to synthesize the μ-controller by reducing the order from 44 to 22 with balanced-realization model reduction. In the meanwhile, a 21-order H_∞ controller with same weightings is also designed via mixed sensitivity method [18] for comparison. These two controllers are implemented in experiments, respectively, and the vibration control effects are evaluated from the curve of power spectrums.

Fig. 6(a) and (b) shows curves of power spectrum of the plate $C(s)$ with and without control measured at locations S-1 and S-2, respectively. It can be seen that peaks of the *first four* modes have been reduced with the use of the μ-synthesis and H_∞ control, meaning that a significant amount of damping can be obtained for these four modes. In addition, comparison of the results between μ-synthesis and H_∞ control further shows that the former is significantly better than the latter. As an example, a further 20 dB reduction for the mode 3 is obtained using μ-synthesis control. As for mode *five*, a little spillover occurs (see Fig. 6(b)). It is due to the model error

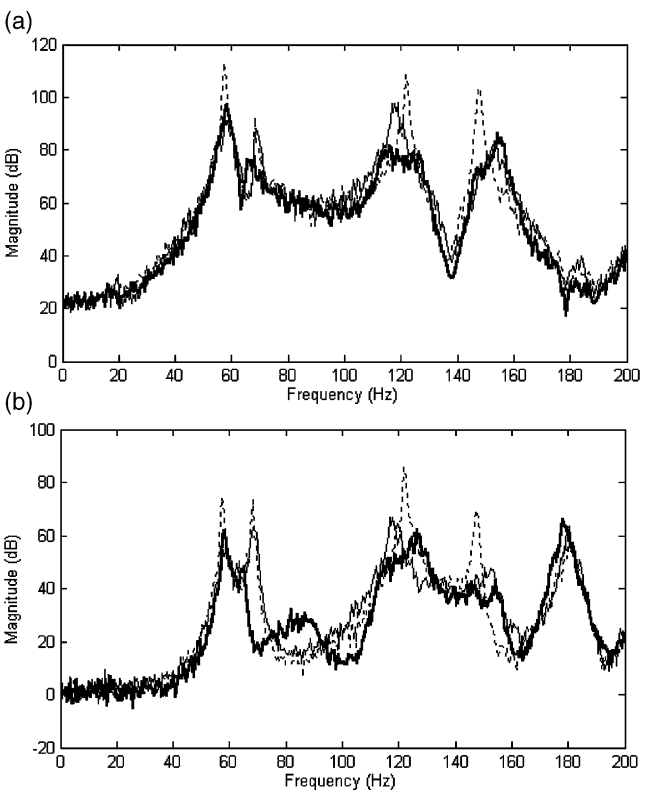

Fig. 6. Curves of power spectrums for the plant $C(s)$ with and without control at (a) S-1 and (b) S-2. Uncontrolled: fine dotted line; μ-synthesis control: thick solid line; H_∞ control: fine solid line.

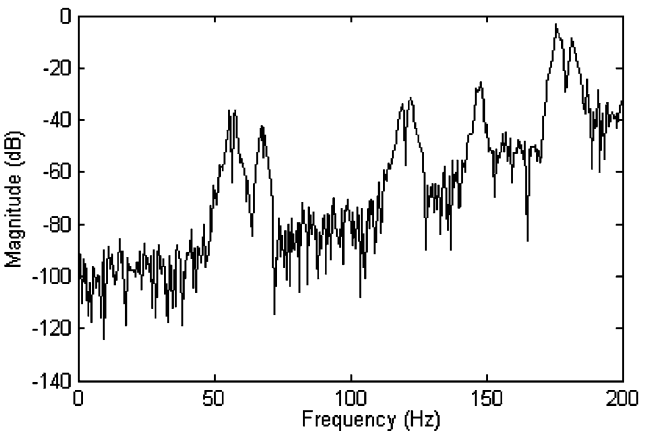

Fig. 7. The model error of system identification.

during system identification, which is illustrated in Fig. 7 by subtracting the maximum singular value of experimental model from that of identified model. It can be seen from Fig. 7 that the model error increases with the frequency increasing from 0 to 200 Hz, and reaches its maximum (−3.24 dB) at 180 Hz (closed to the *fifth* natural frequency, ω_5 = 180.2 Hz) which just exceeds the robust weighting.

Slight changes in mass, stiffens or boundary conditions of the structure will lead to a change of system dynamics. All these changes can be classified as uncertainties and it is very difficult to apprehend, a priori, by the time the controllers are designed. A good control system should then be robust enough when faced with these changes. In order to investigate the robustness of the two control strategies, three masses are added at locations A, B and C of the plate to change modal frequencies so as to simulate parameter variation (see Fig. 3). Their locations and weights are listed in Table 2. As a result of added masses, the nominal model $C(s)$ changes, the *first five* natural frequencies are shifted from 56.6, 68.8, 121.1, 146.5 and 180.2 Hz to 55.6, 67.8, 116.3, 146.0 and 172.8 Hz. It is clear that a small perturbation occurs for natural frequency at modes 1 (−1.77%), 2 (−1.45%) and 4 (−0.3%), whereas a large one at modes 3 (−3.96%) and 5 (−4.1%).

Table 2
Locations and weights of additional masses

Point	x (mm)	y (mm)	Weight (g)
A	205	0	21
B	120	30	21
C	290	−60	10

Fig. 8(a) and (b) shows the power spectrum for the uncertain plate ($C(s)$ + $\Delta C(s)$) with and without control at measuring locations S-1 and S-2, respectively. Again both controllers are applied. It can be seen that for the μ-synthesis, the vibration amplitudes of the *first four* modes are systematically suppressed, while for the H_∞ control, only the amplitudes of modes 1 and 4 have been reduced, while no obvious changes are observed for modes 2 and 3. These results suggest that μ-synthesis is less insensitive to additional masses than H_∞ control is. Evidently, the μ-controller has better robustness than the H_∞ controller. One point to be mentioned is that for mode 5, the control effect is deteriorated due to the large perturbation of natural frequency (-4.1%). Therefore, even for the μ-controller, dynamic changes should be kept with a certain limit.

4. Conclusions

In this paper, the design of a robust μ-controller for vibration suppression of plate-like structures is presented, and the MIMO experimental tests are performed. During

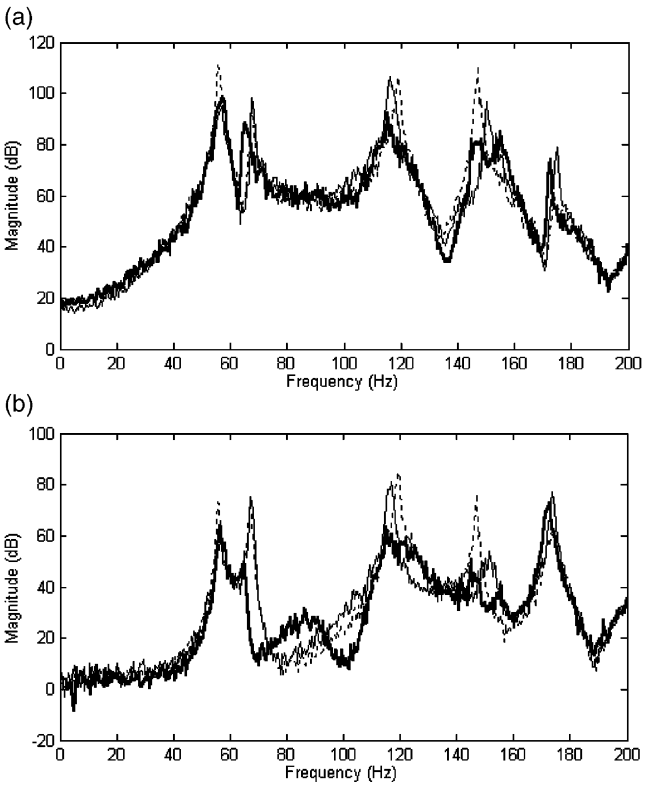

Fig. 8. Curves of power spectrums for the plant ($C(s)$ + $\Delta C(s)$) with and without control at (a) S-1 and (b) S-2. Uncontrolled: fine dotted line; μ-synthesis control: thick solid line; H_∞ control: fine solid line.

the design of μ-controller, the mathematical model between the disturbance force and the structure is not required, and the proper selection of weightings is discussed. In order to investigate the robustness of the synthesized controller for vibration control, the case of parameter variation by adding masses to the structure is studied. Meanwhile, a H_∞ controller with same weightings is also implemented for comparison. From the experimental tests, the following conclusions can be drawn:

1. Based on the presented model, the structural response to disturbance force can be significantly suppressed using both μ-synthesis and H_∞ control techniques. The control performance of μ-synthesis is however better than that of H_∞ control.
2. The perturbation of nominal model weakens the control performance of both designed control approaches. However, μ-synthesis seems to provide a better disturbance rejection in the analyzed bandwidth comparing with H_∞ control, i.e. it is more robust to parameter variation than H_∞ control.

The configuration investigated in this paper, leading to the aforementioned conclusions, is arbitrarily chosen. In this sense, these conclusions are believed to have some general significance for other possible configurations. It should be stressed however, although the design approach presented in this paper is general, the final controller may be significantly different due to the difference in terms of dynamic properties among varied physical systems.

Acknowledgements

The authors would like to thank the Research Committee of the Hong Kong Polytechnic University and the Research Grants Council of Hong Kong Special Administrative Region, China for the financial support to this project (Grant: PolyU 5155/01E).

References

[1] Sadri AM, Wynne RJ, Wright JR. Robust strategies for active vibration control of plate-like structures: theory and experiment. Proceedings of the Institution of Mechanical Engineers Part I—Journal of Systems and Control Engineering 1999;213:489–504.
[2] Hwang JK, Choi CH, Song CK, Lee JM. Robust LQG control of an all-clamped thin plate with piezoelectric actuators/sensors. IEEE/ASME Transactions on Mechatronics 1997;2:205–12.
[3] Li YY, Yam LH. Robust control of vibrating thin plates by mean of variable parameter feedback and model-based fuzzy strategies. Computers and Structures 2001;79:1109–19.
[4] Lee YY, Ng CF. Vibration control of composite plates under random loading using piezoelectric material. Proceedings of the Institution of Mechanical Engineers Part G—Journal of Aerospace Engineering 2000;214:9–25.
[5] Kar IN, Miyakura T, Seto K. Bending the torsional vibration control of a flexible plate structure using H_∞-based robust control law. IEEE Transactions on Control Systems Technology 2000;8:545–53.
[6] Morris JC, Apkarian P, Doyle JC. Synthesis robust mode shapes with μ and implicit model following, control applications. First IEEE Conference on 1992 1992;2:1018–23.

[7] Tani J, Qiu J, Liu Y. Robust control of vortex-induced vibration of a rigid cylinder supported by an elastic beam using μ-synthesis. Journal of Fluids and Structures 1999;13:865–75.
[8] Nonami K, Nishimura H. H_∞/μ Control based frequency shaped sliding mode control for flexible structures. JSME International Journal, Series C 1996;39:493–501.
[9] Hirata M, Liu KZ, Mita T. Active vibration control of a two-mass system using μ-synthesis with a descriptor form representation. Control Engineering Practice 1996;4:545–52.
[10] Balas GJ, Doyle JC. Vibration damping and robust control of the JPL/AFAL experiment using μ-synthesis. In: Proceedings of the 28th Conference on Decision and Control, Tampa, Florida, December. 1989. p. 2689–94.
[11] Balas GJ, Doyle JC. Robustness and performance trade-offs in control design for flexible structures. IEEE Transactions on Control System Technology 1994;2:352–61.
[12] Chang W, Gopinathan SV, Varadan VV, Varadan VK. Design of robust vibration controller for a smart panel using finite element model. ASME Journal of Vibration and Acoustics 2002;124:265–76.
[13] Proulx B, Cheng L. Dynamic analysis of piezoceramic actuation effects on plate vibrations. Thin-Walled Structures 2000;37:147–62.
[14] St-Amant Y, Cheng L. Simulations and experiments on active vibration control of a plate with integrated piezoceramics. Thin-Walled Structures 2000;38:105–23.
[15] Packard A, Doyle JC. The complex structured singular value. Automatica 1993;29:71–109.
[16] Active Control eXperts, Inc. Smart ID system identification software, Cambridge, MA; 1995.
[17] Balas GJ, Doyle JC, Packard A. μ-analysis and synthesis toolbox for use with MATLAB. The Math Works, Natick, MA, 2001.
[18] Doyle JC, Francis BA, Tannenbaum AR. Feedback control theory. New York: Macmillan, 1992.